Accepted Manuscript

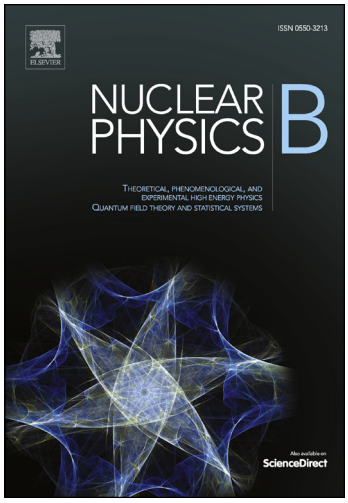

Holographic p-wave superconductor with high-order derivative correction

Jun-Wang Lu, Ya-Bo Wu, Yong Zheng, Li-Gong Mi, Hao Liao

PII: S0550-3213(18)30201-3
DOI: https://doi.org/10.1016/j.nuclphysb.2018.07.015
Reference: NUPHB 14405

To appear in: *Nuclear Physics B*

Received date: 5 April 2018
Revised date: 28 June 2018
Accepted date: 18 July 2018

Please cite this article in press as: J.-W. Lu et al., Holographic p-wave superconductor with high-order derivative correction, *Nucl. Phys. B* (2018), https://doi.org/10.1016/j.nuclphysb.2018.07.015

Holographic p-wave superconductor with high-order derivative correction

Jun-Wang Lu[1],* Ya-Bo Wu[2], Yong Zheng[1], Li-Gong Mi[1], and Hao Liao[1]

[1]*School of Physics and Electronics, Qiannan Normal University for Nationalities, Duyun 558000, P. R. China*

[2]*Department of Physics, Liaoning Normal University, Dalian 116029, P. R. China*

Abstract

In the probe limit, we numerically study the holographic p-wave superconductor phase transition in the high-order derivative theory. Concretely, we study the influences of the high-order derivative correction term αRF^2 on the Maxwell complex vector model(MCV) in the five-dimensional AdS black hole and soliton backgrounds, respectively. In the black hole background, the improving correction parameter α increases the critical temperature and thus enhances the conductor/superconductor phase transition. Meanwhile, as the RF^2 correction becomes stronger, the ratio of the energy gap to the critical temperature decreases from 9.858 to 5.995, which obviously deviates from the universal value. In the soliton background, we find that the correction does not affect the critical chemical potential. However, as the correction parameter α increases, the vector condensate grows faster, which might suggest that the improving α enhances the insulator/superconductor in some sense. The location of the second pole of imaginary part of conductivity increases with α, which implies that the energy of the quasiparticle excitation increases with the improving correction. In addition, the effects of α on the superfluid density agree with the one on the critical value as well as the condensate in both models. Furthermore, the critical exponent of condensate and superfluid density near the critical point is always 1/2 and 1, respectively.

PACS numbers: 11.25.Tq, 04.70.Bw, 74.20.-z

Keywords: Gauge/gravity duality; Holographic superconductor;

*E-mail address:lujunwang.2008@163.com

I. INTRODUCTION

The gauge/gravity duality [1] maps a strong-coupled system to a weak gravity, which thus provides us a feasible and efficient approach for studying the system involving the strong interaction. Since its proposition, it has been widely used in many research area, such as quantum critical point, QCD phase diagram, Non-Fermi liquid, hydrodynamics [2, 3], topological insulator, momentum relaxation [4, 5], quantum Hall effect, especially the high temperature superconductors [6–8].

Since the first holographic s-wave conductor/superconductor was numerically built in the four-dimensional Schwarzschild anti-de Sitter(SAdS) black hole in the probe limit [6], the holographic model was extended to p-wave and d-wave conductor/superconductors and their corresponding insulator/superconductor models [9–13] as well as the analytical methods(Sturm-Liouville eigenvalue approach and matching method) [14, 15]. Moreover, the original probe limit was also generalized to the case including the backreaction from the matter field to the gravitational background [16, 17].

Even though, some obvious deficiencies come to light. For example, the real part of conductivity always vanishes in the lower frequency and lower temperature region, which is forbidden from the well known field theory because of the existence of Goldstone boson in the broken phase. After analysis, this phenomena is ascribed to the large N limit in the gauge/gravity duality, where the high-order derivative corrections are suppressed in the $1/N$ form [16]. Thus, it is necessary to study the effect beyond the large N limit, which is usually realized by introducing some high-order derivative correction terms, such as the pure gravity part(Gauss-Bonnet gravity, Topological gravity and Lifshitz gravity) [18–25], pure gauge field(Born-Infeld nonlinear electrodynamics, exponential electrodynamics and power-Maxwell field) [26–32] and the interaction form of two part(Weyl tensor or Ricci tensor coupled with the gauge field strength) [33–37]. The results showed that the Weyl correction enhances the s-wave and SU(2) p-wave conductor/superconductor phase transition. However, it does not affect the s-wave insulator/superconductor phase transition. Most interestingly, it inhibits the SU(2) p-wave insulator/superconductor phase transition [36, 37].

Besides the Weyl correction, the authors of Ref. [38] proposed another kind of higher derivative correction(the so called αRF^2 correction) to obtain the frequency-dependent conductivity in the neutral black hole. Soon after, Ref. [39] calculated the transport properties at finite density by considering the backreaction of U(1) gauge field and found that both bounds of hydromechanics are violated by the αRF^2 correction. In addition, the s-wave conductor/superconductor phase transition with the RF^2 correction was constructed in Ref. [40]. It is observed that the larger correction enhances the superconductor phase transition and results in a larger deviation from the expected

ratio of the energy gap to the critical temperature, especially, it also enlarges the condensate gap, which is obvious different from the Weyl correction as well as the Gauss-Bonnet correction. Considering the interesting effects of the αRF^2 correction on the s-wave superconductor, it is helpful to study how the αRF^2 correction affects the new p-wave superconductor phase transition consisted of a Maxwell complex vector (MCV) field. Indeed, the MCV p-wave superconductor model was primitively proposed to realize the magnetic field-induced conductor/superconductor phase transition in Ref. [41]. Subsequently, the MCV model was extended to the electric field-induced superconductor model [42, 43] and the corresponding insulator/superconductor model [44, 45] as well as the case including the backreaction from the matter field [46–50]. Especially, it was shown that the MCV model is a generalization of the SU(2) p-wave model with a mass. Meanwhile, in order to investigate the effects of finite N case, the superconductor model was constructed in Lifshitz gravity [51, 52] and Gauss-Bonnet gravity [53] as well as the model with Born-Infeld electrodynamics [54] and Weyl correction[55]. What is the most interesting is that the Weyl correction does not affect the MCV p-wave insulator/superconductor model, which is different from its effect on the SU(2) p-wave model.

Motivated by the above mentioned, we will study systematically the p-wave superconductor phase transition by coupling the MCV field in the AdS black hole and soliton background with the RF^2 correction, respectively, and study the effects of high-order correction on the condensate, critical value, grand potential, the energy gap as well as the superfluid density. For the black hole background, the increasing correction enhances the phase transition. Moreover, the condensate gap decreases and then increases with the increasing correction. Meanwhile, the ratio of the energy gap frequency to the critical temperature decreases with the correction parameter from 9.858 to 5.995, which obviously deviates from the universal value 8. For the soliton background, the high-order derivative correction does not affect the critical chemical potential, while the location of the second pole of imaginary part of conductivity increases with the increasing correction parameter. In addition, for both models, the correction effects on the grand potential, conductivity as well as the superfluid density are consistent with the ones on the condensate.

The organization of this paper is as follows. In Sec. II, in the probe limit, we numerically study the holographic p-wave conductor/superconductor phase transition in the five-dimensional SAdS black hole background coupled to the MCV field with the RF^2 correction, and thus calculate the conductivity and the superfluid density. Similar to the process in Sec. II, the insulator/superconductor phase transition is studied in the AdS soliton background in Sec. III. The final section is devoted to conclusions and discussions.

II. CONDUCTOR/SUPERCONDUCTOR PHASE TRANSITION

In this section, we study the vector condensate in the five-dimensional SAdS black hole, and calculate the frequency dependent conductivity.

The five-dimensional SAdS black hole is of the form [9]

$$\begin{aligned} ds^2 &= -f(r)dt^2+\frac{dr^2}{f(r)}+r^2(dx^2+dy^2+dz^2), \\ f(r) &= r^2\left(1-\frac{r_+^4}{r^4}\right), \end{aligned} \tag{1}$$

where r_+ represents the location of the horizon satisfying $f(r_+)=0$.

Following Ref. [41], we consider the matter action including a Maxwell field, αRF^2 term and a complex vector field

$$\begin{aligned} \mathcal{S}_m = \frac{1}{16\pi G_5}\int dx^5\sqrt{-g}\Big(&-\frac{1}{4}F_{\mu\nu}F^{\mu\nu}+\alpha L^2(R_{\mu\nu\rho\sigma}F^{\mu\nu}F^{\rho\sigma}-4R_{\mu\nu}R^{\mu\rho}F^{\nu}_{\rho}+RF^{\mu\nu}F_{\mu\nu}) \\ &-\frac{1}{2}(D_\mu\rho_\nu-D_\nu\rho_\mu)^\dagger(D^\mu\rho^\nu-D^\nu\rho^\mu)-m^2\rho_\mu^\dagger\rho^\mu+iq\gamma\rho_\mu\rho_\nu^\dagger F^{\mu\nu}\Big), \end{aligned} \tag{2}$$

where $F_{\mu\nu}=\nabla_\mu A_\nu-\nabla_\nu A_\mu$ is the strength of the U(1) gauge field A_μ, and $D_\mu=\nabla_\mu-iqA_\mu$, while m and q corresponds to the mass and the charge of the vector field ρ_μ. The terms $\alpha L^2(R_{\mu\nu\rho\sigma}F^{\mu\nu}F^{\rho\sigma}-4R_{\mu\nu}R^{\mu\rho}F^{\nu}_{\rho}+RF^{\mu\nu}F_{\mu\nu})$ represents the RF^2 correction. Following Refs. [38–40], we briefly confine the parameter α to the range $-1/20\leq\alpha\leq 1/4$, which will be further constrained by the frequency-dependent conductivity in the conductor/superconductor model. Moreover, we do not consider the magnetic field effects on the superconductor phase transition, so the last term with the constant γ is ignored, which characterizes the strength of interaction between ρ_μ and $F_{\mu\nu}$. Meanwhile, compared with the SAdS gravity, we regard the matter sector (2) as a probe where the equations of motion related to the vector field and the gauge field decouple from the equations of gravitational sector and the main physical results are believed to be still grasped.

Varying the action (2) with respect to the vector ρ_μ and the gauge field A_μ, respectively, we can obtain the equations of motion

$$D^\nu(D_\nu\rho_\mu-D_\mu\rho_\nu)-m^2\rho_\mu+iq\gamma\rho^\nu F_{\nu\mu} = 0, \tag{3}$$

$$\begin{aligned} \nabla_\mu\Big(&F^{\mu\nu}-\alpha L^2(4R^{\mu\nu\rho\sigma}F_{\rho\sigma}-8R^{\mu\alpha}F_{\alpha}{}^{\nu}+8R^{\nu\alpha}F^{\mu}_{\alpha}+4RF^{\mu\nu}) \\ &-iq\gamma(\rho^\mu\rho^{\nu\dagger}-\rho^\nu\rho^{\mu\dagger})\Big)+iq(\rho_\mu^\dagger\rho^{\mu\nu}-\rho_\mu\rho^{\mu\nu^\dagger}) = 0. \end{aligned} \tag{4}$$

To construct the p-wave superconductor induced by the gauge field, we take the ansatzs for the vector field ρ_μ and the gauge field A_μ as the following form

$$\rho_\nu dx^\nu = \psi_x(r)dx, \qquad A_\nu dx^\nu=\phi(r)dt, \tag{5}$$

with other components vanishing. Choosing $\psi_x(r)$ and $\phi(r)$ as real functions and substituting the above ansatzs (5) into Eqs. (3) and (4), we can read off the equations for ψ_x and ϕ

$$\psi_x''(r)+\left(\frac{f'(r)}{f(r)}+\frac{1}{r}\right)\psi_x'(r)+\frac{\left(\phi(r)^2-m^2f(r)\right)}{f(r)^2}\psi_x(r) = 0, \tag{6}$$

$$\left(\frac{24\alpha f(r)}{r^2}+1\right)\phi''(r)+\frac{3\left(r\left(8\alpha f'(r)+r\right)+8\alpha f(r)\right)}{r^3}\phi'(r)-\frac{2\psi_x(r)^2}{r^2f(r)}\phi(r) = 0, \tag{7}$$

where the prime denotes the derivative with respect to r. Obviously, for the special case $\alpha = 0$, Eqs. (6) and (7) agree with Eq. (23) in Ref. [48]. Moreover, Eq. (7) is not identical with Eq. (36) in Ref. [55], from which we can believe the present model will generalize some new characters of superconductor. To solve the above equations, we should impose the boundary conditions. At the horizon, the vector field ψ_x is required to be regular, while the gauge field A_μ should satisfy the condition $\phi(r_+) = 0$ to ensure the finite form of $g^{\mu\nu}A_\mu A_\nu$. Near the infinite boundary, the general expansions of the matter field and the gauge field are given by

$$\psi_x(r) = \frac{\psi_{x-}}{r^{\Delta_-}}+\frac{\psi_{x+}}{r^{\Delta_+}}+\ldots, \tag{8}$$

$$\phi(r) = \mu-\frac{\rho}{r^2}+\ldots, \tag{9}$$

where $\Delta_\pm = 1\pm\sqrt{m^2+1}$ with the Breitenlohner-Freedman(BF) bound of the mass $m^2 \geq m_{BF}^2 = -1$. According to the gauge/gravity duality, the coefficients of the leading term ψ_{x-} and the subleading term ψ_{x+} are interpreted as the source and the vacuum-expectation value of the boundary operator $\hat{J}_x$, while μ and ρ are regarded as the chemical potential and the charge density in the dual field theory, respectively. To guarantee the spontaneous breaking of U(1) gauge symmetry in the system, we require that the source of the condensate vanishes, i.e., $\psi_{x-} = 0$.

There is an important symmetry in the above system with the form

$$(r,T)\to\lambda(r,T),\psi_{x+}\to\lambda^{\Delta+1}\psi_{x+},\mu\to\lambda\mu,\rho\to\lambda^3\rho \tag{10}$$

with the positive constant λ. By using Eq. (10) we can fix the chemical potential μ of the system and thus work in the grand canonical ensemble.

Next, we solve the above nonlinear ordinary differential equations. In the present work, we focus on the effects of the high-order derivative corrections(i.e., the parameter α) on the critical temperature and the vector condensate, so we will fix the scaling dimension of the boundary operator $\Delta_+ = \Delta = 2$ throughout the present paper. As a special case, we plot the condensate with $\alpha = 0.15$ as a function of the temperature on the left panel of Fig. 1, from which we find that there is a critical temperature $T_c = 0.10021\mu$, below which the vector field begins to condense.

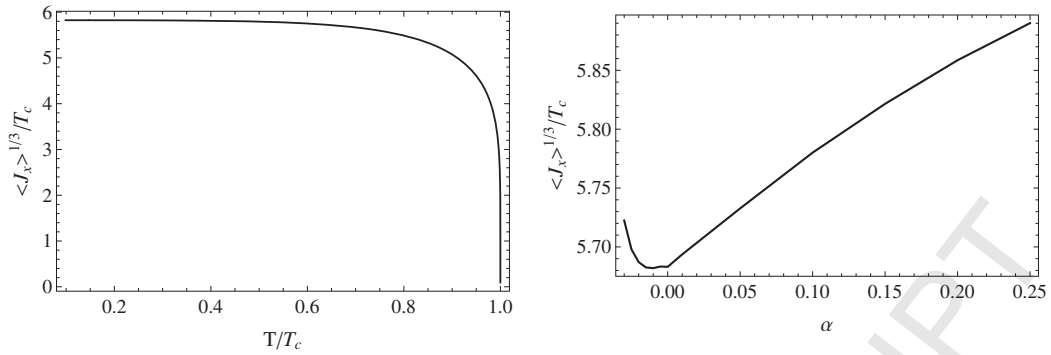

FIG. 1: The condensate versus temperature for $\Delta = 2$ and $\alpha = 0.15$(left) and the condensate gap as a function of the correction parameter α (right).

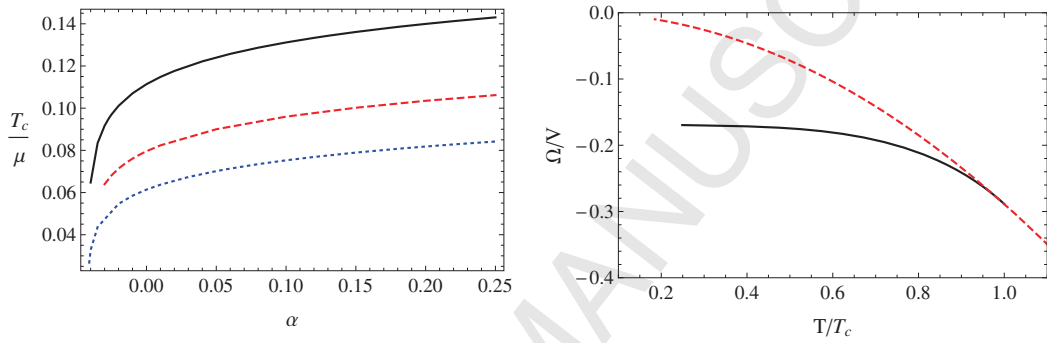

FIG. 2: The critical temperature versus correction parameter α with $\Delta = 3/2$ (black solid),$\Delta = 2$(red dashed), $\Delta = 5/2$(blue dotted)(left) and the grand canonical potential versus temperature in the case of $\alpha = 0.15$ and $\Delta = 2$(right), where the red dashed line and the black solid line correspond to the normal state and the condensate state, respectively.

Moreover, near the critical point, the square root dependence of the vector condensate on the temperature indicates that the critical exponent 1/2 is universal in the probe limit, and thus suggests that the system undergoes a second-order phase transition as expected from the mean field theory. What is more, as the temperature decreases gradually, the condensate tends to be a stable constant, i.e., the condensate gap forms in the low temperature limit.

To study roundly the effects of the high-order derivative correction, we consider the behaviors of vector condensate with different parameter α and obtain the similar behavior. In particular, the condensate gap and the critical temperature as a function of the correction parameter α are plotted on the right panel in Fig. 1 and the left panel in Fig. 2, respectively. It is obvious that for all values of α considered in the work, the critical temperature increases with the increasing α, which indicates that the increasing correction enhances the conductor/superconductor phase transition. In this regard, the effect of α on the critical temperature is similar to the one of Weyl

term [55]. Moreover, when the correction parameter α increases, the condensate gap decreases to a minimum at $\alpha = 0$, and then increases in the case of $\alpha > 0$.

To check the order of the phase transition at the critical point and the stability of the state with vector field condensed below the critical temperature, we calculate the grand potential, which is identified with the Hawking temperature timing the Euclidean on-shell action of the bulk solution. In our case, because we work in the probe limit, we need only consider the contribution from the matter field. Meanwhile, if we further consider the source free condition, there is no necessary to add the counter term to the action. The Euclidian action is given by

$$\begin{aligned} S_{on} &= \int dx^5\sqrt{-g}\Big(-\frac{1}{2}\nabla_\mu(A_\nu F^{\mu\nu}) + \alpha L^2(2\nabla_\mu(A_\nu R^{\mu\nu\rho\sigma}F_{\rho\sigma}) - 4\nabla_\mu(A_\rho R^{\mu\nu}F_\nu{}^\rho) \\ &\quad +4\nabla_\mu(A_\rho R^{\rho\nu}F_\nu{}^\mu) + 2\nabla_\mu(RA_\nu F^{\mu\nu})) - \nabla_\mu(\rho^\dagger_\nu\rho^{\mu\nu})\Big) \\ &\quad +\frac{1}{2}\int dx^5\sqrt{-g}A_\nu\Big(iq\gamma\nabla_\mu(\rho^\mu\rho^{\nu\dagger} - \rho^\nu\rho^{\mu\dagger}) - iq(\rho^\dagger_\mu\rho^{\mu\nu} - \rho_\mu\rho^{\mu\nu^\dagger})\Big) \\ &= \frac{V_3}{T}\Big((1+24\alpha)\mu\rho - \int_{r_0}^{\infty}\frac{r\phi^2\psi^2}{f}dr\Big) \end{aligned} \tag{11}$$

where we have neglected the factor $1/16\pi G_5$ and taken into account the expansions of the matter field at the boundary as well as the integration $\int dtdx^3 = \frac{V_3}{T}$. Introducing the new variable $z = r_+/r$, the density of the grand potential reads

$$\frac{\Omega}{V_3} = \frac{-TS_{on}}{V_3} = -(1+24\alpha)\mu\rho + \int_\epsilon^1 \frac{\phi^2\psi^2}{z(1-z^4)}dz. \tag{12}$$

Considering the numerical integration with $\alpha = 0.15$, we show the density of grand potential as a function of the temperature for the normal state as well as the condensed state in right plot of Fig. 2. It is obvious that with the decreasing temperature, the curve corresponding to the hair state spreads smoothly from the curve of the normal state, which means that at the critical point, the system undergoes a second order phase transition. Moreover, when the temperature falls off the critical value, the curve with vector hair is always below the one without vector hair, which indicates that below the critical temperature, the superconductor state is indeed thermodynamically stable.

As we all know, the conductivity also provides the typical signal to distinguish the state is either in the superconducting sate or not. What is more important, we can read off the energy gap from the frequency dependent conductivity and thus explore the strength of the interaction in the system, so it is helpful for us to study the conductivity. To obtain the conductivity, which is related to the retarded Green function, $\sigma(\omega) = G^R(\omega, k = 0)/i\omega$, we can calculate the perturbation of the gauge field based on the state with vector hair in the gravity spacetime from holography [6]. It should be noted that below the critical temperature, the condensate of the vector operator

$\hat{J}_x$ breaks the U(1) gauge symmetry as well as the rotational symmetry, therefore, it is natural that the conductivity along the condensate direction is different from that perpendicular to the condensate direction. From the calculation for the conductivity along the condensate direction in Ref. [10], one can imagine the perturbation of the gauge field along the x direction is rather complicated. For simplicity, following Refs. [8, 41, 54], we focus on our calculations perpendicular to the superconducting direction with the ansatz $\Delta A_\mu = A_y(r)e^{-i\omega t}$. Substituting the ansatz into Eq. (4), the linearized equation of the perturbation A_y is of the form

$$\left(\frac{8\alpha f'(r)}{r}+\frac{8\alpha f(r)}{r^2}+1\right)A_y''(r)+\left(\frac{8\alpha\omega^2 f'(r)}{rf(r)^2}+\frac{8\alpha\omega^2}{r^2 f(r)}-\frac{2\psi(r)^2}{r^2 f(r)}+\frac{\omega^2}{f(r)^2}\right)A_y(r)$$
$$\left(\frac{8\alpha f''(r)}{r}+\frac{16\alpha f'(r)}{r^2}+\frac{8\alpha f'(r)^2}{rf(r)}+\frac{f'(r)}{f(r)}-\frac{8\alpha f(r)}{r^3}+\frac{1}{r}\right)A_y'(r) = 0, \quad (13)$$

which is similar to the corresponding equations in Refs. [6, 10]. At the horizon, the retarded Green function G^R corresponds to the ingoing wave condition, therefore, $A_y(r)$ can be expressed as

$$A_y(r) = (r-r_+)^{-i\omega/4\pi T}\left(1+A_{y1}(r-r_+)+A_{y2}(r-r_+)^2+A_{y3}(r-r_+)^3+\cdots\right). \quad (14)$$

At the boundary $r\to\infty$, the general falloff of $A_y(r)$ reads

$$A_y(r) = A^{(0)}+\frac{A^{(2)}}{r^2}+\frac{A^{(0)}\omega^2}{2}\frac{log\Lambda r}{r^2}+\cdots. \quad (15)$$

According to the gauge/gravity duality, the Green function G^R can be calculated from the gauge field perturbation, which has the form

$$G^R = (1+24\alpha)\left(\frac{2A^{(2)}}{A^{(0)}}+\omega^2\left(log\Lambda r-\frac{1}{2}\right)\right). \quad (16)$$

Obviously, there is a logarithmic divergence term in the Green function as well as the conductivity, which can be canceled by the holographic renormalization. The conductivity can be expressed as

$$\sigma(\omega) = \frac{G^R}{i\omega} = (1+24\alpha)\frac{1}{i\omega}\left(\frac{2A^{(2)}}{A^{(0)}}-\frac{\omega^2}{2}\right). \quad (17)$$

Note that the correction parameter α appears in the formula of conductivity, which is different from the Weyl correction in Ref. [35] and the RF^2 correction in the s-wave model in Ref. [40]. The frequency dependent conductivity with $\alpha = 0.15$ at the temperature $T/T_c \approx 0.1$ is plotted on the left hand of Fig. 3, from which we can obtain the following results. Firstly, at the zero frequency, there exists a pole in the imaginary part of the conductivity, which corresponds to a delta function of the real part from the Kramers-Kronig(KK) relation. Secondly, there exists a minimum at nonzero frequency for the imaginary part of conductivity. If we define the ratio of

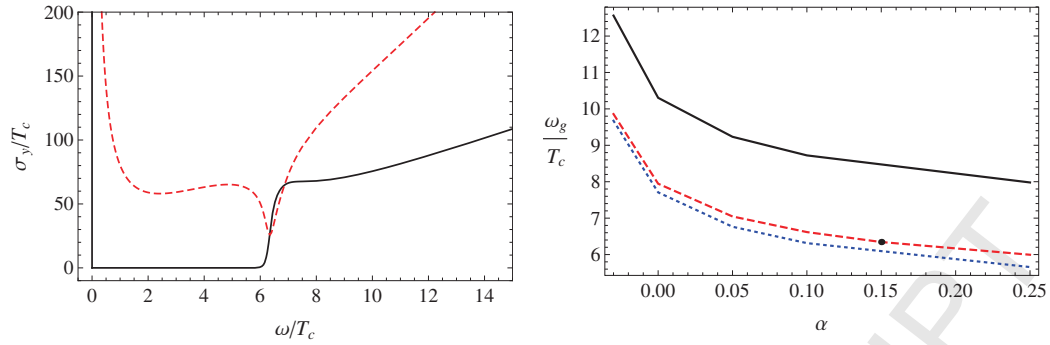

FIG. 3: The AC conductivity versus the frequency in the case of $\alpha = 0.15$ and $\Delta = 2$ (left) and the energy gap as a function of α with $\Delta = 3/2$ (black solid),$\Delta = 2$(red dashed), $\Delta = 5/2$(blue dotted)(right). The curves in both two subplots are obtained near $T/T_c \approx 0.1$.

the energy gap to the critical temperature(ω_g/T_c) as the minimum of the imaginary part of the conductivity($Im[\sigma]$) when $m^2 > m^2_{BF}$[9], we can read off $\omega_g/T_c \approx 6.34$ larger than 3.5 predicted from the BCS theory, which shows the strong interaction in the holographic superconductor model. Thirdly, when the frequency tends to be infinity, both the real and imaginal parts of the conductivity diverge, which might be the general property in the five-dimensional AdS black holes, except for the Lifshitz gravity with the dynamical critical exponent $z > 1$[25]. Meanwhile, we plot the value ω_g/T_c versus the correction parameter α on the right panel of Fig. 3. It is observed that ω_g/T_c decreases with the increasing α, which suggests that the larger correction suppresses the strength of the interaction of holographic system. Moreover, the energy gap is understood as the minimum energy to break the cooper pairs, so the smaller ω_g/T_c, the easier for the phase transition, which is consistent with the effects of α on the critical temperature. In addition, when the value of α is small enough($\alpha < -3/100$), the behaviors of the critical temperature, the condensate as well as the grand potential seem to be reliable, but the reasonable and acceptable conductivity can not be obtained no matter how to adjust the computational accuracy, so it is believed that the holographic superconductor model proposes a new lower limit for the RF^2 correction to some extent. As a result, we mainly consider the case of $-3/100 \leq \alpha \leq 1/4$ in the present paper.

In addition to the conductivity, we calculate the superfluid density below the critical temperature, which is identified by the coefficient of the pole in $Im[\sigma]$ at $\omega = 0$. The result shows that at the critical temperature, the superfluid density n_s arises with the linear depending on the temperature, which agrees with the mean field theory. Meanwhile, as the temperature decreases, the superfluid density saturates a stable value, which matches well with the two-fluid theory about superconductivity. By fitting the superfluid density near the critical point and the zero temperature

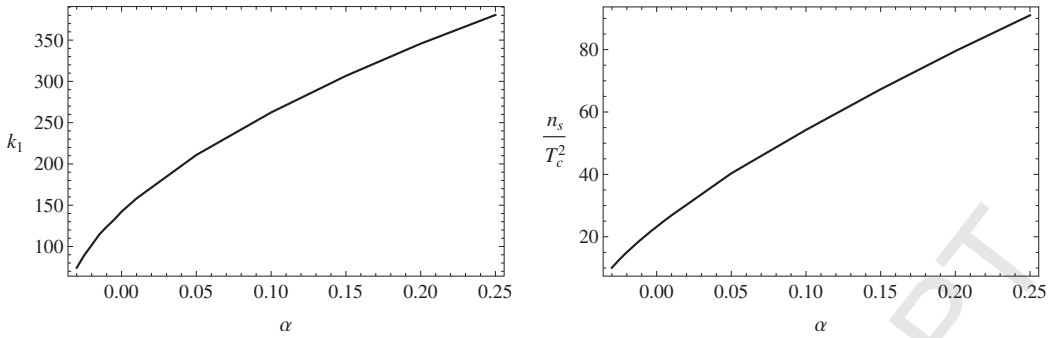

FIG. 4: The coefficient k_1 fitting the superfluid density formula $n_s(T \approx T_c) \sim k_1\sqrt{1-T/T_c}$ near $T \approx T_c$ (left) and the stable value of superfluid density near $T/T_c \approx 0.1$ with the different RF^2 parameter α in the case of $\Delta = 2$.

limit, we can obtain the coefficient k_1 of the fitting formula $n_s \approx k_1(1-T/T_c)$ as well as the stable value of the superfluid $n_s(T \approx 0)$ for various correction parameter α. The α dependent k_1 and $n_s(0)$ for $\Delta = 2$ are plotted on the left and right panel of Fig. 4, respectively. It is observed that both k_1 and $n_s(0)$ increase with α, which means that the superfluid grows faster when we increase the correction parameter α and thus the larger correction enhances the phase transition.

III. INSULATOR/SUPERCONDUCTOR PHASE TRANSITION

In this section, we construct the insulator/superconductor phase transition and thus study how the correction parameter α influences the vector condensate and the conductivity. First of all, the standard five-dimensional AdS soliton reads

$$\begin{aligned} ds^2 &= -r^2dt^2 + \frac{dr^2}{r^2 f(r)} + r^2(dx^2 + dy^2 + f(r)d\chi^2), \\ f(r) &= r^2\left(1 - \frac{r_0^4}{r^4}\right), \end{aligned} \tag{18}$$

which is obtained from the double Wick rotation to the SAdS black hole(1), i.e., $t \to i\chi$ and $z \to it$. To distinguish the soliton from the SAdS black hole in Sec. II, we denote r_0 as the tip, which satisfies the condition $f(r_0) = 0$. To avoid a potential conical singularity at the tip, we impose the periodicity Γ on the spatial direction χ with $\chi \to \chi + \pi/r_0$, i.e., $\Gamma = \pi/r_0$. As for the present soliton background, there is no event horizon, thus no temperature exists. Moreover, because of the existence of the tip, there exists an IR cutoff for the dual field theory, which indicates a confined phase and is thus similar to the mass gap in the insulator phase[12]. Therefore, it is believed that the present soliton system can be used to model the insulator/superconductor phase transition [12, 21, 53].

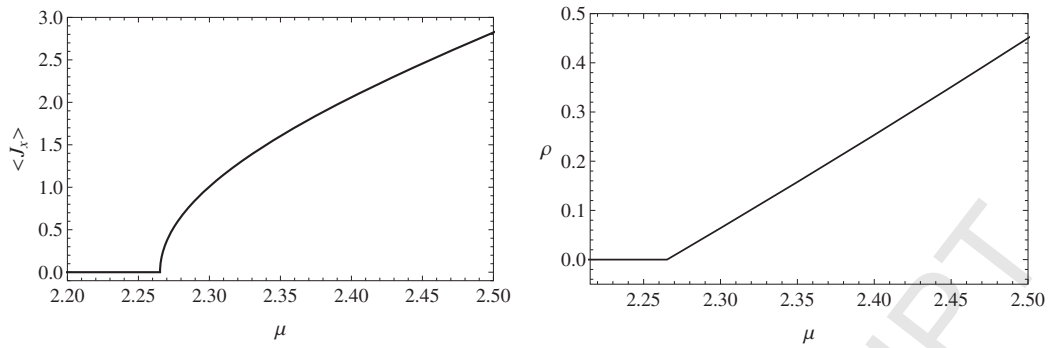

FIG. 5: The condensate(left) and the charge density(right) as a function of the chemical potential in the case of $\Delta = 2$.

Now, we construct a new p-wave insulator/superconductor phase transition with RF^2 correction. For the matter field, we take the action the same as the one of the conductor/superconductor phase transition, i.e., the action(2). Naturally, the form of the gauge field and the matter field is taken as Eq. (5). By varying the action(2) with respect to ρ_μ and A_μ, we can obtain the equations of motion in the background (18) as

$$\psi_x''(r) + \left(\frac{f'(r)}{f(r)} + \frac{1}{r}\right)\psi_x'(r) + \frac{\phi(r)^2 - m^2 r^2}{r^2 f(r)}\psi_x(r) = 0, \tag{19}$$

$$\left(\frac{8\alpha f'(r)}{r} + \frac{8\alpha f(r)}{r^2} + 1\right)\phi''(r) + \Big(\frac{1+8\alpha f''(r)}{r} + \frac{16\alpha f'(r)}{r^2} + \frac{8\alpha f'(r)^2 + r f'(r)}{r f(r)} - \frac{8\alpha f(r)}{r^3}\Big)\phi'(r) - \frac{2\psi_x(r)^2\phi(r)}{r^2 f(r)} = 0. \tag{20}$$

Obviously, Eqs. (19) and (20) with $\alpha = 0$ are the same with Eq. (11) in Ref. [48] when one neglects the backreaction. However, the above equations are different from the ones with Weyl correction in Ref. [55].

To numerically solve these equations, we impose the boundary conditions at both the tip and the infinite boundary. At the tip, the Neumann-like boundary condition is required to ensure $\psi_x(r_0)$ and $\phi(r_0)$ to be regular, while near the infinity, the general falloffs of $\psi_x(r)$ and $\phi(r)$ are of the forms (8) and (13), respectively. Moreover, the interpretations of the coefficients ψ_{x-}, ψ_{x+}, μ and ρ are the same as that in the black hole from the gauge/gravity dual dictionary. By means of the symmetry of the system, $r \to \lambda r, \psi_x \to \lambda\psi_x, \phi \to \lambda\phi, \Gamma \to \lambda^{-1}\Gamma$, hereafter we will take the periodicity $\Gamma = \pi$ by rescaling the vector field ψ_x and the gauge field ϕ. By calculations, we show the condensate(the charge density) as a function of the chemical potential with $\alpha = 0.15$ on the left (right) panel of Fig. 5, from which we find that there exists a critical chemical potential $\mu_c = 2.26523$, beyond which both the vector condensate and the charge density arise. By fitting the condensate near the critical potential, we still find the squared condensate dependent on the

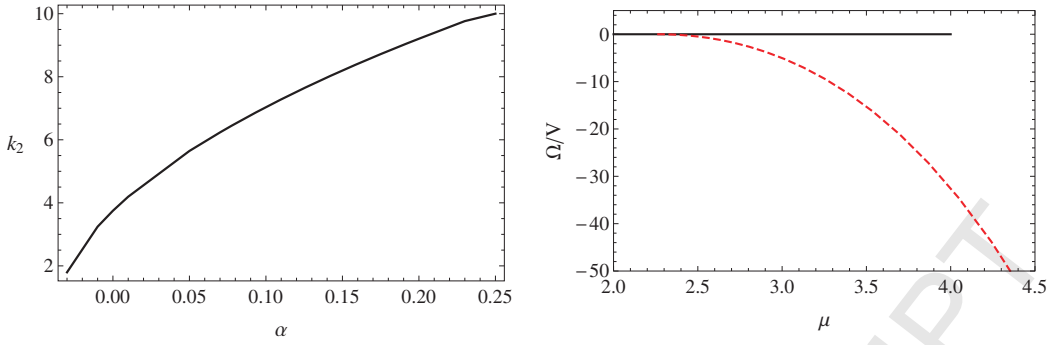

FIG. 6: The coefficient k_2 of the fitting formula $\langle \hat{J}_x \rangle (\mu \approx \mu_c) \sim k_2 \sqrt{\mu/\mu_c - 1}$ near $\mu \approx \mu_c$ (left) and the density of grand potential Ω/V for both normal state(black solid) and condensate state(red dashed) with $\alpha = 0.15$(right).

chemical potential, which means that a second order phase transition occurs at the critical point. Moreover, we also fit the charge density, it is found that the critical exponent of the charge density is 1. To see intuitively the effect of α on holographic model, we calculate the case of different correction parameter α. The results show that the critical chemical potential is independent of the correction parameter α, which tells us that the correction might not affect the stability of the AdS soliton system.

To study further the effect of high-order derivative correction on the vector condensate, we plot the coefficient k_2 of the fitting formula $\langle \hat{J}_x \rangle (\mu \approx \mu_c) \sim k_2 \sqrt{\mu/\mu_c - 1}$ as a function of correction parameter α on the left plot of Fig. 6. Obviously, the coefficient increases with the correction parameter, which implies that the larger the correction is, the faster the condensate grows. In this sense, the larger correction enhances the growth of the condensate. Moreover, to check the order of the phase transition near the critical point, we define a "temperature" of the soliton system and then calculate the grand potential by the on-shell action of matter field, which is displayed on the right plot of Fig. 6. It is easily observed that near the critical chemical potential, the red dashed curve corresponding to the vector condensate state appears smoothly from the black solid curve corresponding to the normal state. Meanwhile, the value of grand potential for the condensate state is always lower than the one for the normal state when the chemical potential increases beyond the critical value. This implies that at the critical point, the system indeed undergoes a second-order phase transition and at the larger chemical potential, the condensate state is thermodynamically favored.

Then, we calculate the conductivity in the five-dimensional AdS soliton with the vector hair. Here, we still take the gauge perturbation perpendicular to the direction of the condensate, i.e.,

$\Delta A = A_y(r)e^{-i\omega t}$, with other components vanishing, from which one can read off the linearized equation of the perturbation as

$$\left(\frac{8\alpha f'(r)+r}{r}+\frac{8\alpha f(r)}{r^2}\right)A_y''(r)+\Big(\frac{8\alpha f''(r)+r}{r}+\frac{16\alpha f'(r)}{r^2}+\frac{8\alpha f'(r)^2}{rf(r)}+\frac{f'(r)}{f(r)} -\frac{8\alpha f(r)}{r^3}\Big)A_y'(r)+\left(\frac{4\alpha\omega^2 f''(r)}{r^2 f(r)}+\frac{8\alpha\omega^2 f'(r)}{r^3 f(r)}-\frac{2\psi(r)^2}{r^2 f(r)}+\frac{\omega^2}{r^2 f(r)}\right)A_y(r)=0. \quad (21)$$

To numerically solve the differential equation, we impose the boundary conditions. Near the tip $r = r_0$, the expansion of $A_y(r)$ still includes the logarithmic term. In order to ensure the perturbation to be finite, we require the Neumann-like boundary condition to eliminate the logarithmic divergence, which is similar to the boundary condition of the gauge field ϕ, thus the concrete form of $A_y(r)$ reads

$$A_y(r) = 1 + A_{y1}(r - r_+) + A_{y2}(r - r_+)^2 + A_{y3}(r - r_+)^3 + \cdots , \quad (22)$$

while at the boundary $r \to \infty$, the expansion of $A_y(r)$ can be expressed as

$$A_y(r) = A^{(0)} + \frac{A^{(2)}}{r^2} + \frac{A^{(0)}\omega^2}{2}\frac{log\Lambda r}{r^2} + \cdots . \quad (23)$$

Therefore, the conductivity is given by

$$\sigma(\omega) = \frac{1}{i\omega}\left(\frac{2A^{(2)}}{A^{(0)}} - \frac{\omega^2}{2}\right), \quad (24)$$

where the logarithmic divergence term in the general falloff of $A_y(r)$ is removed by the holographic renormalization.

On the left hand of Fig. 7, we shows the imaginary part of conductivity as a function of the frequency in the case of $\alpha = 0.15$ with $\mu/\mu_c \approx 2$. Obviously, beyond the critical chemical potential, there exists a pole (corresponding to a delta function in the real part of $\sigma(\omega)$) at the zero frequency, which is expected from the standpoint of the superconductor. Moreover, as we all know, the location of the second pole corresponds to the energy of the quasiparticle excitation. To see intuitively how the high-order derivative correction affects the holographic model, we plot the energy of quasiparticle excitation k_3 as a function of the parameter α with $\mu/\mu_c \approx 2$ on the right hand of Fig. 7, from which we find that when the parameter α increases, the location of the second pole of $Im[\sigma_y]$, which means that the energy of the quasiparticle excitation increases with the improving high-order derivative correction.

In addition to the conductivity, by extracting the coefficient of the pole in $Im[\sigma_y]$ at $\omega = 0$, we obtain the superfluid density, which is plotted on the left panel of Fig. 8. The result shows that

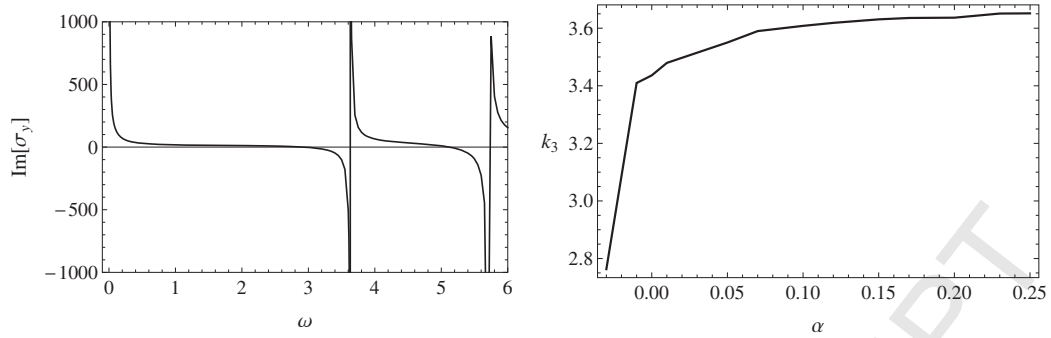

FIG. 7: The imaginary part of the AC conductivity versus the frequency in the case of $\alpha = 0.15$ with $\mu/\mu_c \approx 2$(left) and the location k_3 of the second pole of $Im[\sigma_y]$ as a function of the correction parameter α with $\mu/\mu_c \approx 2$(right).

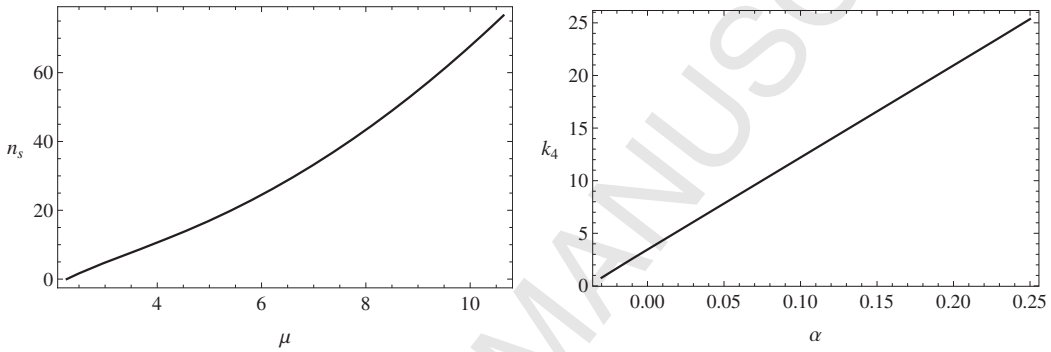

FIG. 8: The superfluid density versus the chemical potential with $\alpha = 0.15$(left) and the coefficient k_4 of the formula $n_s \sim k_4(1 - \mu/\mu_c)$ by fitting the superfluid density near the critical chemical potential(right).

as we increase the chemical potential above the critical value, the superfluid density appears as the linear behavior dependent on the chemical potential, which is consistent with the mean field theory. Furthermore, we also plot the coefficient k_4 of the fitting formula $n_s \sim k_4(1 - \mu/\mu_c)$ about the superfluid density with respect to the parameter α on the right panel of Fig. 8. It is observed that when the high-order derivative correction become larger, the superfluid density grows faster, which agrees with the effect of the correction on the vector condensate.

IV. CONCLUSIONS AND DISCUSSIONS

So far, we have numerically constructed the p-wave superconductors with the high-order derivative correction in the probe limit. Concretely, we mainly studied the effects of the high-order terms αRF^2 on the conductor/superconductor and insulator/superconductor phase transition, respectively, and further observed the transport phenomenon for the superconductor. The main

conclusions can be summarized as follows.

In terms of the conductor/superconductor phase transition in the five-dimensional AdS black hole, the critical temperature increases with the parameter α, which indicates that the stronger correction αRF^2 enhances the phase transition. However, the improving dimension of the vector operator Δ makes the phase transition more difficult. This is reasonable, because the larger Δ corresponds to the larger "mass" in the dual field theory. When the temperature decreases gradually from the critical value, the vector condensate tends to be a stable value(the so called condensate gap). Moreover, the condensate gap decreases with the increasing parameter α until $\alpha \approx 0$, whereafter, it increases with the increasing α. This non-monotonic behavior of condensate gap with respect to α is not only different from the one for the s-wave case with RF^2 correction [40], but also unlike the MCV p-wave model with Weyl correction [55]. The reason for the difference between the RF^2 term and Weyl term for the superconductor model is still unclear, which need deep analysis. In addition, in the case with the vector "hair", we observed a delta function of the real part of conductivity at zero frequency. Besides, we found the ratio of the energy gap to the critical temperature ω_g/T_c decreases from 9.858 to 5.995 with the range $\alpha \in [-3/100, 1/4]$, which obviously deviates from the universal value 8. Even though, ω_g/T_c is always larger than the BCS value 3.5 for all the value of α, which implies that the holographic model indeed involves the strong interaction.

As for the insulator/superconductor model, the critical chemical potential does not depend on the high-order derivative correction. Moreover, the critical chemical potential with $\Delta = 5/2$ is larger than the one with $\Delta = 3/2$ when the αRF^2 correction is fixed. Meanwhile, we studied the frequency dependent conductivity. It is observed that the location of the second pole of the imaginary part moves toward right with the increasing α, which indicates that the energy of the quasiparticle excitation increases with α. In addition, we read off the superfluid density, which increases with the increasing chemical potential. However, it does not tend to a stable value, which is unlike the one in the conductor/superconductor model.

For both superconductor models, near the critical point, the critical exponent of the charge density is 1, which agrees with the mean field theory. What is more, the critical exponent of the vector condensate near the critical value is 1/2. This means that the system undergoes a second-order phase transition, which is verified by the behavior of the grand potential.

In a word, the increasing high-order derivative correction α enhances the conductor/superconductor phase transition but not affect the critical chemical potential of the insulator/superconductor phase transition. Near the critical point, both systems undergo a second-order

phase transition. The stable value of the vector condensate increases with the larger α in the AdS black hole. The ratio of the energy gap to the critical value much larger than the BCS value indicates the holographic models indeed simulate the strong interaction. Therefore, our results shed light on understanding the strong interacting system from the perspective of the gravity/gauge duality to some extent.

However, it should be noted that we have only numerically constructed the superconductor model in the probe limit where the rich phase structure was likely covered up [46–48, 54]. Meanwhile, we have not calculated the critical value via the analytical method such as the Sturm-Liouville method [14] as well as the Matching method. To systematically study the effects of α on the MCV model, it is meaningful to calculate superconductor model by the Sturm-Liouville method as well as by including the backreaction from the MCV field. Moreover, as a "toy" model, we simply adopted the range of correction parameter as $-1/20 \leq \alpha \leq 1/4$. In order to systematically study the holographic model in the five-dimensional case with αRF^2 correction, we will try to constrain the range of the parameter α by demanding that the dual CFT respects micro-causality or examining if there are any unstable modes of the gauge field in the bulk for various α [38, 56, 57]. Furthermore, by introducing a Weyl correction into the Einstein-Maxwell-Axion theory in four-dimensional spacetime, Ref. [58] realized the metal-insulator phase transition at zero temperature. Due to the similar effects between the Weyl term and the RF^2 term on the superconductor, it is interesting to study how the RF^2 term induces the metal-insulator phase transition, which is our future work.

Acknowledgments

We would like to thank Prof. Q. Y. Pan and Z. Y. Nie for their helpful discussion and comments. This work is supported in part by NSFC (Nos.11475143, 11647167, 11747615 and 11575075), Foundation of Guizhou Educational Committee(Nos. Qianjiaohe KY Zi [2016]311 Zi) and the Foundation of Scientific Innovative Research Team of Education Department of Guizhou Province (201329).

[1] J. M. Maldacena, Adv. Theor. Math. Phys. **2**, 231 (1998) [hep-th/9711200].

[2] Z. Y. Fan, Phys. Rev. D **97**, no. 6, 066013 (2018) [arXiv:1801.07870 [hep-th]].

[3] Y. Bu, R. G. Cai, Q. Yang and Y. L. Zhang, arXiv:1803.08389 [hep-th].

[4] Y. Ling, Int. J. Mod. Phys. A **30**, no. 28-29, 1545013 (2015).

[5] Y. Ling, C. Niu, J. Wu, Z. Xian and H. b. Zhang, Phys. Rev. Lett. **113**, 091602 (2014) [arXiv:1404.0777 [hep-th]].

[6] S. A. Hartnoll, C. P. Herzog and G. T. Horowitz, Phys. Rev. Lett. **101**, 031601 (2008) [arXiv:0803.3295 [hep-th]].

[7] R. G. Cai, L. Li, Y. Q. Wang and J. Zaanen, Phys. Rev. Lett. **119**, no. 18, 181601 (2017) [arXiv:1706.01470 [hep-th]].

[8] R. G. Cai, L. Li, L. F. Li and R. Q. Yang, Sci. China Phys. Mech. Astron. **58**, no. 6, 060401 (2015) [arXiv:1502.00437 [hep-th]].

[9] G. T. Horowitz and M. M. Roberts,Phys. Rev. D **78**, 126008 (2008) [arXiv:0810.1077 [hep-th]].

[10] S. S. Gubser and S. S. Pufu, JHEP **0811**, 033 (2008) [arXiv:0805.2960 [hep-th]].

[11] Z. Y. Nie, Q. Pan, H. B. Zeng and H. Zeng, Eur. Phys. J. C **77**, no. 2, 69 (2017) [arXiv:1611.07278 [hep-th]].

[12] T. Nishioka, S. Ryu and T. Takayanagi, JHEP **1003**, 131 (2010) [arXiv:0911.0962 [hep-th]].

[13] G. Liu and Y. Peng, Mod. Phys. Lett. A **30** (2015) 34, 1550183.

[14] G. Siopsis and J. Therrien,JHEP **1005**, 013 (2010) [arXiv:1003.4275 [hep-th]].

[15] H. F. Li, R. G. Cai and H. Q. Zhang, JHEP **1104**, 028 (2011) [arXiv:1103.2833 [hep-th]].

[16] S. A. Hartnoll, C. P. Herzog and G. T. Horowitz, JHEP **0812**, 015 (2008) [arXiv:0810.1563 [hep-th]].

[17] G. T. Horowitz and M. M. Roberts, JHEP **0911**, 015 (2009) [arXiv:0908.3677 [hep-th]].

[18] Z. H. Li, Y. C. Fu and Z. Y. Nie, Phys. Lett. B **776**, 115 (2018) [arXiv:1706.07893 [hep-th]].

[19] S. Mukhopadhyay and C. Paul, Int. J. Mod. Phys. A **33**, no. 01, 1850002 (2018).

[20] A. Sheykhi, A. Ghazanfari and A. Dehyadegari, Eur. Phys. J. C **78**, no. 2, 159 (2018) [arXiv:1712.04331 [hep-th]].

[21] Q. Pan, J. Jing and B. Wang, JHEP **1111**, 088 (2011) [arXiv:1105.6153 [gr-qc]].

[22] X. M. Kuang, W. J. Li and Y. Ling, JHEP **1012**, 069 (2010) [arXiv:1008.4066 [hep-th]].

[23] C. J. Luo, X. M. Kuang and F. W. Shu, Phys. Lett. B **759**, 184 (2016) [arXiv:1605.03260 [hep-th]].

[24] J. W. Lu, Y. B. Wu, J. Xiao, C. J. Lu and M. L. Liu, Int. J. Mod. Phys. A **31**, no. 19, 1650110 (2016).

[25] J. W. Lu, Y. B. Wu, P. Qian, Y. Y. Zhao and X. Zhang, Nucl. Phys. B **887**, 112 (2014) [arXiv:1311.2699 [hep-th]].

[26] Y. Liu, Y. Gong and B. Wang, JHEP **1602**, 116 (2016) [arXiv:1505.03603 [hep-ph]].

[27] W. Yao and J. Jing, Phys. Lett. B **759**, 533 (2016) [arXiv:1603.04516 [gr-qc]].

[28] C. Y. Zhang, Y. B. Wu, Y. N. Zhang, H. Y. Wang and M. M. Wu, Nucl. Phys. B **914**, 446 (2017) [arXiv:1609.09318 [hep-th]].

[29] S. Pal and S. Gangopadhyay, Annals Phys. **388**, 472 (2018) [arXiv:1708.06240 [hep-th]].

[30] D. Ghorai and S. Gangopadhyay, Eur. Phys. J. C **76**, no. 3, 146 (2016) [arXiv:1511.02444 [hep-th]].

[31] X. Y. Guo, L. C. Zhang and R. Zhao, Mod. Phys. Lett. A **29**, no. 19, 1450083 (2014).

[32] S. l. Cui and Z. Xue, Phys. Rev. D **88**, no. 10, 107501 (2013) [arXiv:1306.2013 [hep-th]].

[33] Y. Ling and X. Zheng, Nucl. Phys. B **917**, 1 (2017) [arXiv:1609.09717 [hep-th]].

[34] S. A. Hosseini Mansoori, B. Mirza, A. Mokhtari, F. L. Dezaki and Z. Sherkatghanad, JHEP **1607**, 111 (2016) [arXiv:1602.07245 [hep-th]].

[35] J. P. Wu, Y. Cao, X. M. Kuang and W. J. Li, Phys. Lett. B **697**, 153 (2011) [arXiv:1010.1929 [hep-th]].

[36] Z. Zhao, Q. Pan and J. Jing, Phys. Lett. B **719**, 440 (2013) [arXiv:1212.3062 [hep-th]].

[37] D. Momeni, N. Majd and R. Myrzakulov, EPL **97**, no. 6, 61001 (2012) [arXiv:1204.1246 [hep-th]].

[38] R. C. Myers, S. Sachdev and A. Singh, Phys. Rev. D **83**, 066017 (2011) [arXiv:1010.0443 [hep-th]].

[39] R. G. Cai and D. W. Pang, Phys. Rev. D **84**, 066004 (2011) [arXiv:1104.4453 [hep-th]].

[40] Z. Zhao, Q. Pan, S. Chen and J. Jing, Chin. Phys. Lett. **30**, no. 12, 121101 (2013) [arXiv:1301.3728 [gr-qc]].

[41] R. G. Cai, S. He, L. Li and L. F. Li, JHEP **1312**, 036 (2013) [arXiv:1309.2098 [hep-th]].

[42] D. Wen, H. Yu, Q. Pan, K. Lin and W. L. Qian, Nucl. Phys. B **930**, 255 (2018) [arXiv:1803.06942 [hep-th]].

[43] Y. B. Wu, J. W. Lu, W. X. Zhang, C. Y. Zhang, J. B. Lu and F. Yu, Phys. Rev. D **90**, no. 12, 126006 (2014) [arXiv:1410.5243 [hep-th]].

[44] R. G. Cai, L. Li, L. F. Li and Y. Wu, JHEP **1401**, 045 (2014) [arXiv:1311.7578 [hep-th]].

[45] M. Rogatko and K. I. Wysokinski, JHEP **1603**, 215 (2016) [arXiv:1508.02869 [hep-th]].

[46] R. G. Cai, L. Li and L. F. Li, JHEP **1401**, 032 (2014) [arXiv:1309.4877 [hep-th]].

[47] L. F. Li, R. G. Cai, L. Li and C. Shen, Nucl. Phys. B **894**, 15 (2015) [arXiv:1310.6239 [hep-th]].

[48] R. G. Cai, L. Li, L. F. Li and R. Q. Yang, JHEP **1404**, 016 (2014) [arXiv:1401.3974 [gr-qc]].

[49] E. Kiritsis and L. Li, JHEP **1601**, 147 (2016) [arXiv:1510.00020 [cond-mat.str-el]].

[50] R. G. Cai and R. Q. Yang, Phys. Rev. D **91**, no. 2, 026001 (2015) [arXiv:1410.5080 [hep-th]].

[51] Y. B. Wu, J. W. Lu, M. L. Liu, J. B. Lu, C. Y. Zhang and Z. Q. Yang, Phys. Rev. D **89**, no. 10, 106006 (2014) [arXiv:1403.5649 [hep-th]].

[52] Y. B. Wu, J. W. Lu, C. Y. Zhang, N. Zhang, X. Zhang, Z. Q. Yang and S. Y. Wu, Phys. Lett. B **741**, 138 (2014) [arXiv:1412.3689 [hep-th]].

[53] Y. B. Wu, J. W. Lu, Y. Y. Jin, J. B. Lu, X. Zhang, S. Y. Wu and C. Wang, Int. J. Mod. Phys. A **29**, 1450094 (2014) [arXiv:1405.2499 [hep-th]].

[54] P. Chaturvedi and G. Sengupta, JHEP **1504**, 001 (2015) [arXiv:1501.06998 [hep-th]].

[55] L. Zhang, Q. Pan and J. Jing, Phys. Lett. B **743**, 104 (2015) [arXiv:1502.05635 [hep-th]].

[56] A. Buchel and R. C. Myers, JHEP **0908**, 016 (2009) [arXiv:0906.2922 [hep-th]].

[57] M. Brigante, H. Liu, R. C. Myers, S. Shenker and S. Yaida, Phys. Rev. D **77**, 126006 (2008) [arXiv:0712.0805 [hep-th]].

[58] Y. Ling, P. Liu, J. P. Wu and Z. Zhou, Phys. Lett. B **766**, 41 (2017) [arXiv:1606.07866 [hep-th]].